ELSEVIER

Journal of Biomechanics 37 (2004) 721–729

JOURNAL OF BIOMECHANICS

www.elsevier.com/locate/jbiomech
www.JBiomech.com

Analysis of oscillatory flow disturbances and thermal characteristics inside fluidic cells due to fluid leakage and wall slip conditions

A.-R.A. Khaled[a], K. Vafai[b,*]

[a] Department of Mechanical Engineering, The Ohio State University, Columbus, OH 43210, USA
[b] Department of Mechanical Engineering, University of California, A363 Bourns Hall, Riverside, CA 92521-0425, USA

Accepted 14 September 2003

Abstract

The effects of both fluid leakage and wall slip conditions are studied analytically and numerically on the fluctuation rate in the flow inside non-isothermal disturbed thin films supported by soft seals within a fluidic cell. Flow disturbances due to internal pressure pulsations and external squeezing are considered in this work. The main controlling parameters are found to be the dimensionless leakage parameter, softness of the seal, squeezing number, dimensionless slip parameter, the thermal squeezing parameter and the power law index. Accordingly, their influences on the fluctuation rate and heat transfer characteristics inside disturbed thin films are determined and discussed. It is found that an increase in the dimensionless leakage parameter, softness of the seal-upper plate assembly and the wall slip parameter result in more cooling and an increase in the fluctuation level in the flow. However, an increase in the squeezing number and the fluid power index decrease flow fluctuations. Finally, a suggested design to alleviate a number of problems in fluidic cells is presented.

Keywords: Thin films; Fluidic cell; Squeezing; Non-Newtonian fluid; Seals; Leakage; Fluid slip

1. Introduction

Thin films are utilized in various chemical and biological systems such as in novel biosensing devices (Lavrik et al., 2001). These novel sensors have the advantage to accurately, quickly, and economically screen patients for the presence of various diseases or can be used to detect many bio-warfare agents. A primary form of these sensors is the microcantilever detector, which is based on the deflection of its free end that is caused by the imposed stresses at one of its surfaces. This surface stress is due to the reaction between the analyte's molecules flowing with the working fluid inside the thin film and the special coating, called receptor, on that active surface.

Examples of reactions in biomolecular (receptor/analyte) applications which occur within a fluidic cell are: antibody–antigen (receptor/analyte) bindings or DNA hybridization of a pair of DNA strands (receptor/analyte) having complementary sequences. An application of antibody–antigen bindings is the binding of polyclonal anti-PSA (prostate-specific antigen) antibody and free PSA (fPSA). This binding is important in discovering the prostate cancer (Wu et al., 2001). In many cases, there exist disturbances in the flow which can disturb the deflection of the microcantilever and produce a noise in the measurement (Fritz et al., 2000).

Part of the noise in the measurement is ascribed due to the fact that oscillations in the flow may produce an oscillatory drag force on the microcantilever surface causing it to vibrate. In the experimental work of Fritz et al. (2000), they reported a 100 nm deflection in the microcantilever due to initial flow disturbances in the fluidic cell while the microcantilever deflection due to receptor/analyte binding was of the order of 10 nm. Meanwhile, flow oscillations may change the microcantilever temperature causing it to produce an additional noise as the microcantilever is composed of two layers (bimaterial) having different coefficients of thermal expansion. Fritz et al. (2000) also reported a

*Corresponding author. Tel.: +1-909-787-2135; fax: +1-909-787-2899.
E-mail address: vafai@engr.ucr.edu (K. Vafai).

0021-9290/$ - see front matter © 2003 Elsevier Ltd. All rights reserved.
doi:10.1016/j.jbiomech.2003.09.017

50 nm deflection of the microcantilever due to its bimetallic effect. This was five times the microcantilever deflection due receptor/analyte binding. The rate of receptor/analyte binding changes with the flow velocity as demonstrated in the experimental work of Pritchard et al. (1995). As such, flow oscillations add extra noise due to surface stresses. It is critical to minimize flow oscillations in designing fluidic cells.

Flow disturbances can be due to external disturbances or due to internal pressure pulsations when the pumping process is irregular. Even a small change in the internal pressure of the fluidic cell can have a substantial impact since the thickness of the thin film is very small. This fact is more pronounced if the thin film is supported by soft seals. Accordingly, the dynamics and thermal characterization of thin films will be altered producing a noise in the biosensor measurement which is proportional to the fluctuation rate in the flow. Another source for flow disturbances is the flow leakage which can seriously affect the operation of the microcantilever (Raiteri et al., 2000).

Several authors analyzed flow inside oscillatory disturbed thin films like Langlois (1962). In addition, many authors considered in their analysis laminar pulsating flows like Hemida et al. (2002). Recently, Khaled and Vafai (2002) studied effects of internal pressure pulsations on oscillatory squeezed laminar flow and heat transfer inside thin films supported by soft seals. However, the literature lacks an investigation of the effects of fluid leakage on pulsating flow and heat transfer inside thin films in the presence of soft seals as it represents an important source for flow disturbances.

Another motivation for this study is to analyze flow inside disturbed fluidic cells under wall slip conditions with different fluid types in order to determine their best operating conditions that cause minimum flow fluctuations. It is worth noting that wall slip conditions can be achieved either when the fluid contains suspensions or when the plates are coated with water repellent resigns (Watanabe and Udagawa, 2001). Also, slip occur when the size of the thin film is so small that the Kundsen number, a ratio of the molecular mean free path to the characteristic length of the cell, is between 10^{-3} and 10^{-1} as for flow of gases in microchannels (Shiping and Ameel, 2001). This work will analyze analytically and numerically flow and heat transfer associated with side leakage, wall slip condition and non-Newtonian effects inside disturbed thin films supported by soft seals in order to obtain better designs of fluidic cells.

2. Analysis

A two-dimensional thin film fluidic cell that has a small thickness h compared to its length $2B$ and its width D is considered. The inlet of this fluidic cell is taken to be at its center forming a symmetrical fluidic cell, Fig. 1(a), in order to assure an almost uniform deformation in the seal along its length under pulsative flows. The analysis will be concerned with one half of the fluidic cell shown in Fig. 1(b) due to the symmetry of the proposed cell. The x-axis is taken along the axial direction starting from the inlet while y- and z-axis are taken along its thickness and width, respectively, as shown in Fig. 1(b).

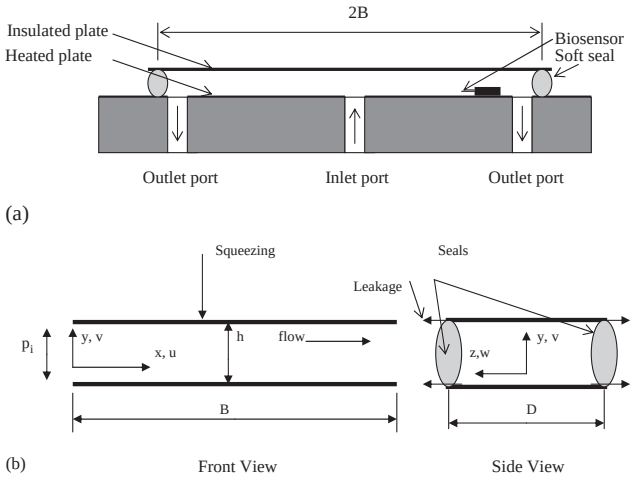

Fig. 1. Schematic diagram of (a) a symmetrical fluidic cell (it has a uniform variation in the film thickness under disturbed conditions and can be used for multi-detection purposes) and (b) corresponding coordinate systems with leakage illustration.

2.1. Fluid leakage in the presence of internal pressure pulsations

The lower plate of the thin film is assumed to be fixed while the upper plate is attached to the lower plate by soft seals. The average dimensionless motion of the upper plate H is expressed according to the following relation:

$$H \equiv \frac{h}{h_0} = (1 + H_p), \tag{1}$$

where h, h_0 and H_p are the dimensional average thin film thickness, a reference thin film thickness and the average dimensionless change in the film thickness due to internal pressure forces, respectively.

The following dimensionless variables will be utilized in the analysis:

$$X = \frac{x}{B}, \tag{2a}$$

$$Y = \frac{y}{h_0}, \tag{2b}$$

$$Z = \frac{z}{B}, \tag{2c}$$

$$\tau = \omega t, \tag{2d}$$

$$U = \frac{u}{(\omega B + V_0)}, \tag{2e}$$

$$V = \frac{v}{h_0 \omega}, \tag{2f}$$

$$W = \frac{w}{(\omega B + V_0)}, \tag{2g}$$

$$\Pi = \frac{p - p_e}{\mu(\omega + V_0/B)\varepsilon^{-2}}, \tag{2h}$$

$$\theta = \frac{T - T_1}{(q_0 h_0)/k}, \tag{2i}$$

where ω, T_1, p_e, V_0, μ, k, and ε are the reference frequency of internal pulsations, inlet temperature of the fluid, a constant representing the exit pressure, a constant representing a reference dimensional velocity, dynamic viscosity of the fluid, thermal conductivity of the fluid and the perturbation parameter ($\varepsilon = h_0/B$), respectively. The pressure at the exit and the outside pressure are assumed to be at the exit pressure. The lower plate is maintained at a uniform wall heat flux condition q_0. The variables t, u, v, w, p and T are the time, axial velocity component, normal velocity component, lateral velocity component, pressure and the temperature, respectively. The dimensionless variables X, Y, Z, τ, U, V, W, Π and θ are the dimensionless forms of x, y, z, t, u, v, w, p and T variables, respectively.

The average dimensionless change in the film thickness is related to the average dimensionless pressure inside the thin film fluidic cell Π_{AVG} through the theory of linear elasticity. It assumes that the change in pressure force on the upper plate is linearly proportional to the average change in the thin film thickness (Boresi et al., 1978), by the following relation:

$$H_p = F_n \Pi_{AVG}, \tag{3}$$

where F_n is named, the fixation parameter. A larger F_n value indicates softer seal-upper plate assembly. The inertia of the upper plate is negligible because the frequency of pulsations is usually small. The fixation parameter F_n that appears in Eq. (3) is equal to

$$F_n = K^* \frac{\mu(V_0 + \omega B)D}{2(B + 0.5D)E\varepsilon^2 h_s}, \tag{4}$$

where E and h_s are the effective modulus of elasticity and the effective dimension of the seal ($h_s = h_0$ for a square seal cross section), respectively. The factor K^* reflects the contribution of the elastic behavior of the upper plate. The parameter F_n becomes apparent when the thin film thickness is very small ($h_0 < 0.15$ mm).

Most flows inside thin films possess relatively small Reynolds numbers and could be creep flows as in biological applications. That is the modified Reynolds numbers, $Re_L = V_0 h_0 \varepsilon/\upsilon$ and $Re_S = h_0^2 \omega/\upsilon$, are less than one. Therefore, the low Reynolds number flow model is adopted. Accordingly, the continuity and momentum equations for the flow inside the fluidic cell filled with a Newtonian fluid are reduced to the following non-dimensionalized equations along with the non-dimesionalized energy equation:

$$U = \frac{1}{2}\frac{\partial \Pi}{\partial X} H^2 \left(\frac{Y}{H}\right)\left(\frac{Y}{H} - 1\right), \tag{5}$$

$$V = \frac{dH}{d\tau}\left(3\left(\frac{Y}{H}\right)^2 - 2\left(\frac{Y}{H}\right)^3\right), \tag{6}$$

$$W = -\frac{1}{2} M_L \Pi \frac{Z}{H}\left(\frac{Y}{H}\right)\left(\frac{Y}{H} - 1\right), \tag{7}$$

$$\frac{\partial^2 \Pi}{\partial X^2} - \frac{M_L}{H^3}\Pi = \frac{\sigma}{H^3}\frac{dH}{d\tau}, \tag{8}$$

$$P_S\left(\frac{\partial \theta}{\partial \tau} + \frac{12}{\sigma} U \frac{\partial \theta}{\partial X} + V \frac{\partial \theta}{\partial Y}\right) = \frac{\partial^2 \theta}{\partial Y^2}. \tag{9}$$

In this section, no slip conditions are assumed at the lower and the upper plates of the fluidic cell as shown in Eq. (5). The parameters σ and P_S are called the squeezing number and thermal squeezing parameter, respectively. They are defined as

$$\sigma = \frac{12}{1 + V_0/(\omega B)}, \; P_S = \frac{\rho c_p h_0^2 \omega}{k}. \tag{10}$$

According to Eq. (7), the leakage inside the thin film is distributed equally on both sides of the thin film and it is relatively small thus linearization of the lateral pressure gradient is used. As seen in Eq. (7), side leakage is proportional to the pressure difference between internal and external (at P_e) pressures of the thin film. Eq. (8) is the corresponding modified Reynolds equation of the problem. Eq. (9) is applicable at the plane of symmetry at $Z = 0$. The parameter M_L in Eq. (7) will be named the dimensionless leakage parameter. It is related to the total leaked mass m_L through the following relation: $m_L = 1/12 \int_0^1 M_L \Pi \rho D h_0 (V_0 + \omega B)\, dX$. The inlet pressure due to flow disturbances in the pumping process is considered to have the following relation:

$$\Pi_i = \Pi_0(1 + \beta_v \sin(\gamma \omega t)), \tag{11}$$

where β_v, γ, Π_i and Π_0 are the dimensionless amplitude in the pressure, dimensionless frequency of the pressure pulsations, inlet dimensionless pressure and the mean dimensionless inlet pressure, respectively. The solution

to Eq. (8) is obtained as

$$\Pi(X,\tau)=\left(\Pi_{\mathrm{i}}+\frac{\sigma}{M_{\mathrm{L}}}\frac{\mathrm{d}H}{\mathrm{d}\tau}\right)\cosh\left(\sqrt{\frac{M_L}{H^3}}X\right)-\frac{\sigma}{M_{\mathrm{L}}}\frac{\mathrm{d}H}{\mathrm{d}\tau}+\left(\frac{\sigma}{M_{\mathrm{L}}}\frac{\mathrm{d}H}{\mathrm{d}\tau}-\left[\Pi_{\mathrm{i}}+\frac{\sigma}{M_{\mathrm{L}}}\frac{\mathrm{d}H}{\mathrm{d}\tau}\right]\cosh\left(\sqrt{\frac{M_{\mathrm{L}}}{H^3}}\right)\right)\times\frac{\sinh\left(\sqrt{\frac{M_{\mathrm{L}}}{H^3}}X\right)}{\sinh\left(\sqrt{\frac{M_{\mathrm{L}}}{H^3}}\right)}. \tag{12}$$

The reference velocity V_0 is taken to be the velocity inside the thin film in absence of any disturbance and it is related to Π_0 according to following relation:

$$\Pi_0=12-\sigma \tag{13}$$

2.2. Slip effects and non-Newtonian effects in the presence of external squeezing

In this part, the effects of fluid slip at the boundaries and non-Newtonian effects in the presence of an external disturbance are analyzed. The dimensionless oscillation of upper plate is based on the following generic relationship:

$$H=1-\beta\cos(\gamma\tau), \tag{14}$$

where β and γ are the amplitude of the motion and a selected dimensionless frequency, respectively. The apparent viscosity μ of a non-Newtonian fluid such as a biofluid at low flow rates can be expressed according to the following power-law formula: $\mu=\mu_0\left|\partial u/\partial y\right|^{n-1}$ where n is a constant representing the power law index. As a result, axial momentum equation for creep flow reduces to the following, μ_0 replaces μ in Eq. 2(h):

$$\frac{\partial\Pi}{\partial X}=\left(\frac{V_0+\omega B}{h_0}\right)^{n-1}\frac{\partial}{\partial Y}\left(\left|\frac{\partial U}{\partial Y}\right|^{n-1}\frac{\partial U}{\partial Y}\right). \tag{15}$$

According to the linear relationship between the wall slip velocity and the shear rate at a solid boundary (Navier, 1823), the dimensionless boundary conditions for the axial velocity at the plates are:

$$U(0,\tau)-\frac{\beta_{\mathrm{P}}}{h_0}\frac{\partial U(0,\tau)}{\partial Y}=0,$$
$$U(H,\tau)+\frac{\beta_{\mathrm{P}}}{h_0}\frac{\partial U(H,\tau)}{\partial Y}=0, \tag{16}$$

where β_{p} is the dimensional slip parameter. By solving Eq. (15) and the continuity equation, the modified Reynolds equation is

$$\frac{\partial}{\partial X}\left[\left(\frac{n}{(2n+1)}+2\left(\frac{\beta_{\mathrm{P}}}{h_0}\right)\frac{1}{H}\right)\left(\frac{H}{2}\right)^{(2n+1)/n}\left(-\frac{\partial\Pi}{\partial X}\right)^{1/n}\right]=-\frac{\sigma}{24}\frac{\mathrm{d}H}{\mathrm{d}\tau}\left(\frac{V_0+\omega B}{h_0}\right)^{(2n+1)/n}. \tag{17}$$

For a constant average inlet velocity condition V_0 during the oscillations, Eq. (15) can be used for determining the velocity field, U and V, for the lower half of the thin film ($Y/H<0.5$). They are found to be

$$U(X,Y,\tau)=\frac{[\sigma\beta\gamma\sin(\gamma\tau)X-(12-\sigma)H(0,\tau)]}{12\left((n/(2n+1))+2\left(\beta_{\mathrm{P}}/h_0\right)1/H\right)H}\times\left[\frac{n}{n+1}\left\{\left(1-2\left(\frac{Y}{H}\right)\right)^{((n+1)/n)}-1\right\}-2\left(\frac{\beta_{\mathrm{P}}}{h_o}\right)\frac{1}{H}\right], \tag{18}$$

$$V(X,Y,\tau)=\frac{\beta\gamma\sin(\gamma\tau)}{(n/(2n+1)+2(\beta_{\mathrm{P}}/h_0)1/H)}\times\left[\frac{n}{n+1}\left\{\left(\frac{n}{2n+1}\right)\left(\frac{1}{2}\right)\times\left\{\left(1-2\left(\frac{Y}{H}\right)\right)^{(2n+1)/n}-1\right\}+\frac{Y}{H}\right\}+2\left(\frac{\beta_{\mathrm{P}}}{h_0}\right)\left(\frac{1}{H}\right)\left(\frac{Y}{H}\right)\right]. \tag{19}$$

Accordingly, the fluid slip velocity at the wall is obtained as

$$U_{\mathrm{Slip}}(X,\tau)=\frac{-2(\beta_{\mathrm{P}}/h_0)\frac{1}{H}}{12(n/(2n+1)+2(\beta_{\mathrm{P}}/h_0)\frac{1}{H})}\times\frac{[\sigma\beta\gamma\sin(\gamma\tau)X-(12-\sigma)H(0,\tau)]}{H}. \tag{20}$$

2.3. Thermal boundary condition

It is assumed that the upper plate is insulated while the lower plate is maintained at a constant heat flux. Accordingly, the dimensionless thermal boundary and initial conditions are

$$\theta(X,Y,0)=0,\ \ \theta(0,Y,\tau)=0,$$
$$\frac{\partial\theta(X,0,\tau)}{\partial Y}=-1,\ \ \frac{\partial\theta(X,H,\tau)}{\partial Y}=0. \tag{21}$$

3. Numerical methods

The dimensionless average thickness of the thin film for the leakage problem was determined by solving

Eqs. (1) and (3) and the average of Eq. (12), simultaneously, using the explicit formulation with respect to time. Accordingly, the velocity field U, V and W was determined. The energy equation, Eq. (9), was then solved using the Alternative Direction Implicit (ADI) method by transferring the problem to one with constant boundaries using the following transformation: $\tau^* = \tau$, $\xi = X$ and $\eta = Y/H$.

4. Results and discussions

The used dimensionless parameters in the leakage problem were selected according to the following data from the literature: the estimated volume of the fluidic cell, Fig. 1(b), is 50 μl and the flow rate of the liquid is 0.5 ml/min. The thin film thickness was taken to be less than 0.15 mm and the effective modulus of elasticity of the seal was considered to be between about 10^5 pa.

4.1. Leakage and slippage effects on flow dynamics inside thin films

It is noticed from Fig. 2(a) that the thin film thickness decreases as the dimensionless leakage parameter M_L increases. A relief in the average internal pressure is expected when the leakage rate increases at a constant inlet pressure. This reduced pressure result in a reduction in the force holding the upper plate thus the thickness decreases. Accordingly, the absolute values of the inlet pressure gradient increases as the leakage rate increases, Fig. 2(b). This causes the inlet flow rate to increase.

According to Fig. 2(a), the leakage rate has almost an insignificant effect on the fluctuation rate at the upper plate, $dH/d\tau$. However, the associated reduction in the film thickness increases fluctuations in axial and normal velocities at the sensor position which tend to magnify the noise in the sensor measurements especially if the sensor is placed near the disturbed plate. Induced lateral flow due to leakage may cause a lateral bending or twisting of the sensor (e.g. microcantilever). Both effects tend to reduce the accuracy of the measurement and may damage the microcantilever over a long period of time. The fluctuations due to mass leakage can be minimized if the fluidic cell width D is maximized.

When the used seal-upper plate assembly is soft as for large F_n values, the film thickness will be more sensitive to internal pressure pulsations. As a result, an increase in the fixation parameter F_n causes an increase in the fluctuation rate at the upper plate (Fig. 3) and

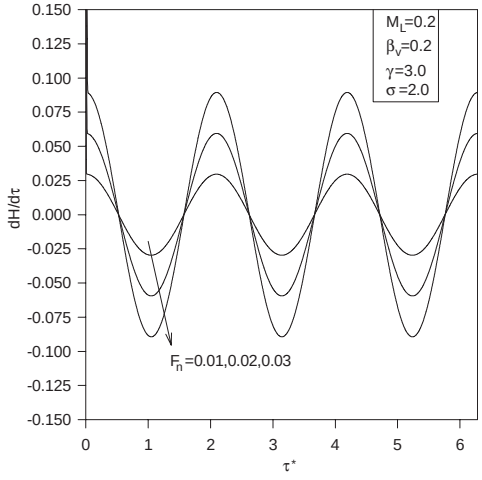

Fig. 3. Effects of the fixation parameter F_n on the fluctuation rate at the upper plate $dH/d\tau$. The fluctuation rate decreases as the seal becomes softer.

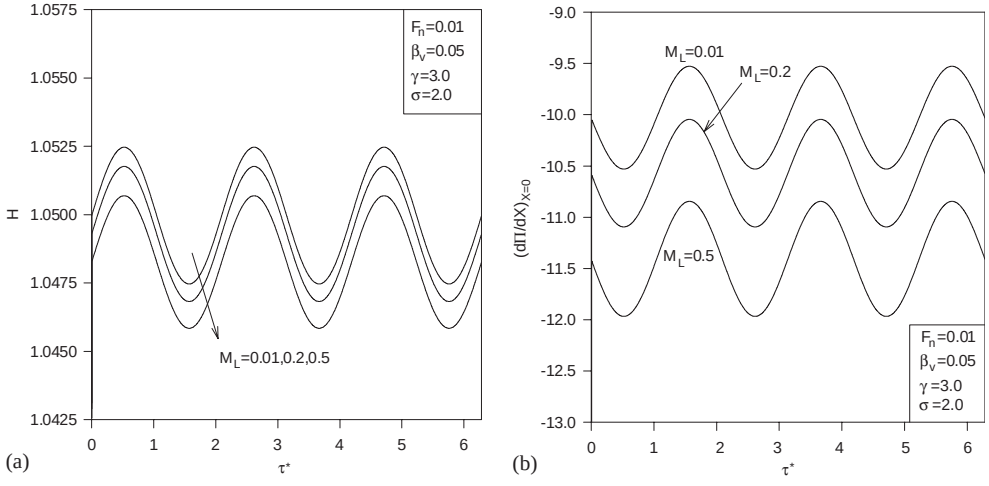

Fig. 2. Effects of the dimensionless leakage parameter M_L on (a) the dimensionless thin film thickness H, and (b) the Inlet Pressure Gradient. The film thickness decreases with an increase in the leakage.

consequently an increase in flow fluctuations is associated (Eqs. (5)–(7) and (12)). Meanwhile, an increase in the squeezing number σ means a reduction in pressure pulsations levels thus a reduction in the fluctuation rate is noticed (Fig. 4). As such, soft sealing assembly and large velocities produce large fluctuations in the flow within the fluidic cell. Similar trends can be extracted for the lateral fluctuations in view of Eq. (7). Accordingly, the noise in the measurement with respect to a microcantilever sensor is magnified for relatively large values of the fixation parameter F_n especially at large pulsation rates.

The resistance against the flow decreases as the dimensionless wall slip parameter β_P/h_0 increases. Thus the wall slip velocity increases as β_P/h_0 increases,

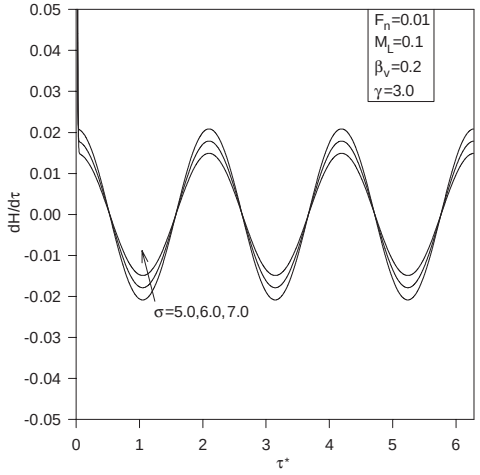

Fig. 4. Effects of the squeezing number σ on the fluctuation rate at the upper plate $dH/d\tau$. The fluctuation rate decreases as the order of the inlet velocity decreases compared to the axial squeezed velocity due to pressure pulsations.

Fig. 5(a). This results in a reduction in the maximum axial velocity since the average flow velocity is kept constant for each case. The maximum slip velocity occurs during the squeezing stages. Due to the increase in the uniformity of the axial velocity profiles as β_P/h_0 increases, flow fluctuations increase near the fixed plate, Fig. 5(b). This causes enlargement in the noise with respect to microcantilever measurements.

Due to the expected increase in wall shear stresses for pseudoplastic ($n<1$) fluids as the power law index n decreases, the wall slip velocity increases as n decreases, Fig. 6(a). The uniformity of the axial velocity profiles increases as n decreases. However, flow fluctuations increase near the fixed plate as n decreases, Fig. 6(b). This indicates that dilute solutions of analytes are preferred over blood and many biofluids in biosensing applications as they produce minimal flow fluctuations near the undisturbed plate.

4.2. Leakage and slippage effects on the thermal characteristics inside thin films

The reduction in internal pressures associated with an increase in the leakage rate results in an increase in the inlet flow rate which reduces the average dimensionless lower plate temperature as seen in Fig. 7. This causes the temperature levels around the microcantilever surface to be closer to the inlet temperature, Eq. 2(i). These temperatures could be quite different from the original microcantilever temperature. Thus, the deflection of the bimaterial microcantilever due to thermal effects is magnified when leakage is present. Similarly, thermal effects on bimaterial sensors can be magnified by an increase in F_n and a decrease in σ since both effects cause a reduction in the dimensionless average lower plate temperature (Figs. 8 and 9). According to Fig. 7,

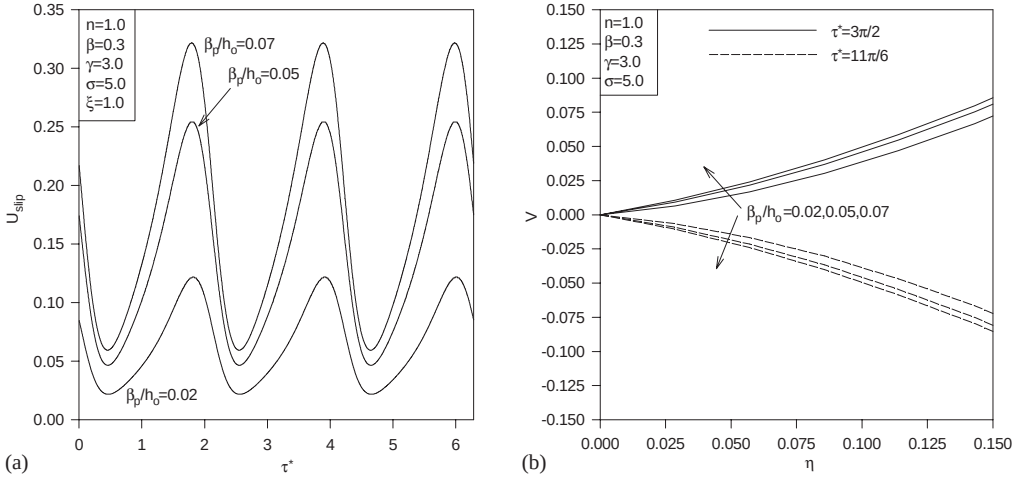

Fig. 5. Effects of the dimensionless slip parameter β_P/h_0 on (a) the dimensionless wall slip velocity U_{slip}, and (b) the dimensionless normal velocity V (the dimensionless time $\tau^* = 3\pi/2$ corresponds to the time at which the fluctuation rate at the upper plate is maximum while $\tau^* = 11\pi/6$ corresponds to the time at which the fluctuation rate at the upper plate is minimum).

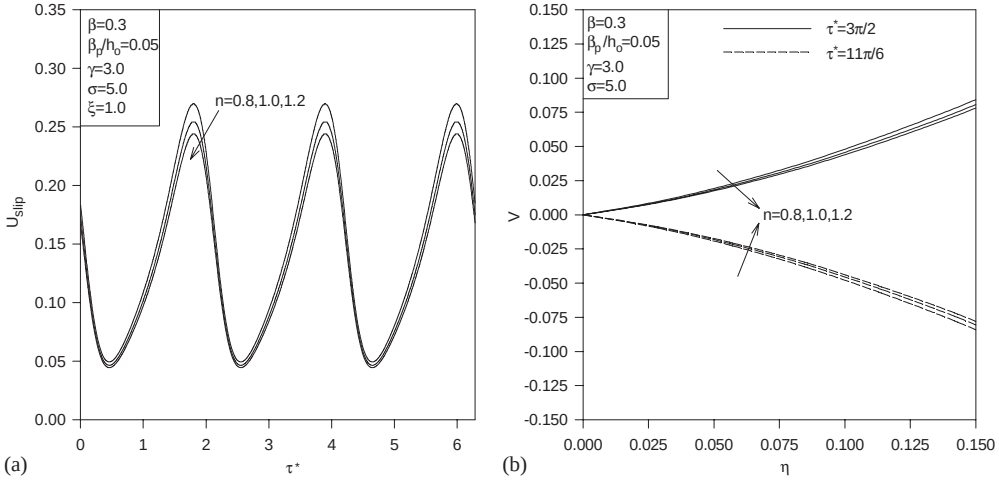

Fig. 6. Effects of the power law index n on (a) the dimensionless wall slip velocity U_{slip}, and (b) the dimensionless normal velocity V (the dimensionless time $\tau^* = 3\pi/2$ corresponds to the time at which the fluctuation rate at the upper plate is maximum while $\tau^* = 11\pi/6$ corresponds to the time at which the fluctuation rate at the upper plate is minimum).

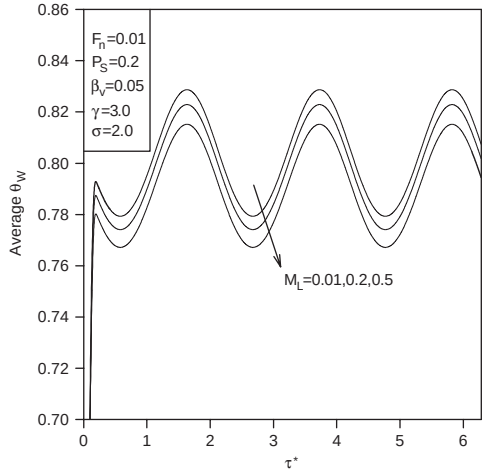

Fig. 7. Effects of the dimensionless leakage parameter M_L on the average dimensionless lower plate temperature θ_W. The cooling increases with an increase in the leakage rate.

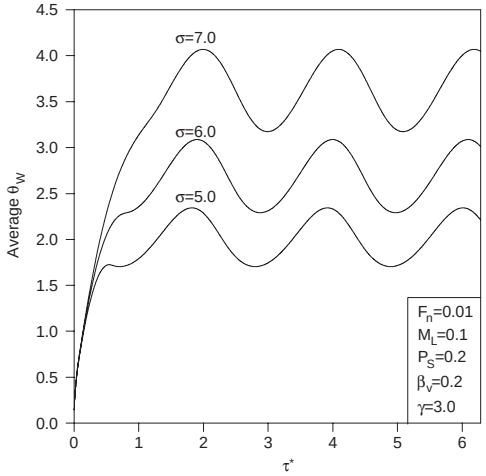

Fig. 9. Effects of the squeezing number σ on the average dimensionless lower plate temperature θ_W. The cooling increases as the order of the inlet velocity increases.

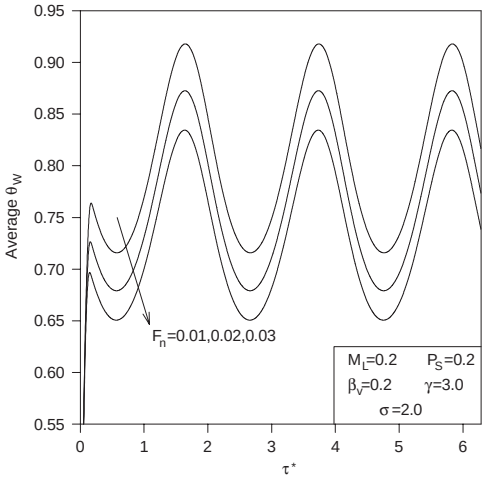

Fig. 8. Effects of the fixation parameter F_n on the average dimensionless lower plate temperature θ_W. The cooling increases as the seal becomes softer.

for the range of M_L used, thermal variations can be neglected when compared to variations in M_L.

5. A design for a thin film fluidic cell

In order to minimize axial, normal and lateral flow disturbances inside thin films, the parameters F_n, m_L and β need to be minimized. Special designs of these films can satisfy these constraints. As an example, the multi-compartment fluidic cell with multiple inlets shown in Fig. 10 will result in reductions in minimizing flow fluctuations associated with internal/external disturbances, leakage and the softening effect of the support and upper plate assembly. That is because the expected reduced pressure difference between the main cell and the two secondary cells minimizes m_L. The width of the

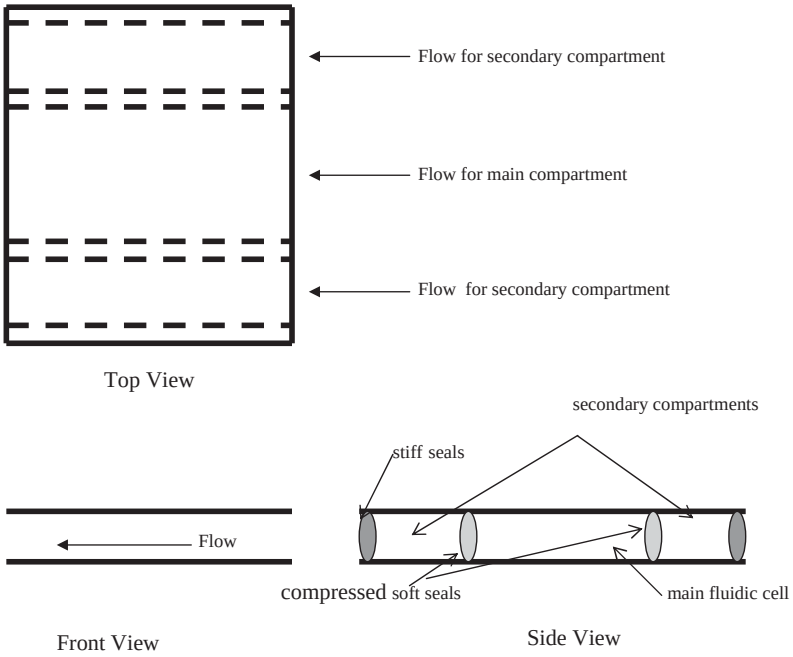

Fig. 10. Multi-compartment fluidic cell.

secondary compartment needs to be less than half of the width of the main cell thus reducing F_n. The parameters F_n and m_L can also be reduced if stiff seals are used for the outer most supports while the interior soft seals are kept under compression as shown in Fig. 10. Thus β is reduced for the suggested design. The flow inside the secondary compartments can be similar to the main flow conditions or separately controlled.

6. Conclusions

Flow fluctuations within a fluidic cell and consequently the noise in the measurement due to flow disturbances, are minimized by considering the following effects:

- minimizing the working velocities;
- maximizing the thickness of the upper plate;
- maximizing the thin film width if relatively large leakage rate is involved;
- minimizing the thin film width in the absence of leakage;
- maximizing the perturbation parameter;
- utilizing dilute working fluid;
- maximizing the thin film thickness.

The last three effects may increase the microcantilever deflection due to thermal effects. As such, the problem of reducing flow oscillations was alleviated by considering new designs for fluid cells can be utilized so that reliable and accurate detections of biological agents can be achieved.

Acknowledgements

We acknowledge partial support of this work by DOD/DARPA/DMEA under grant number DMEA90-02-2-0216.

References

Boresi, A.P., Sidebottom, O.M., Seely, A.B., Smith J, .O., 1978. Advanced Mechanics of Materials. Wiley, New York.

Fritz, J., Baller, M.K., Lang, H.P., Rothuizen, H., Vettiger, P., Meyer, E., Güntherodt, H.–J., Gerber, Ch., Gimzewski, J.K., 2000. Translating biomolecular recognition into nanomechanics. Science 288, 316–318.

Hemida, H.N., Sabry, M.N., Abdel-Rahim, A., Mansour, H., 2002. Theoretical analysis of heat transfer in laminar pulsating flow. International Journal of Heat and Mass Transfer 45, 1767–1780.

Khaled, A.–R.A., Vafai, K., 2002. Flow and heat transfer inside thin films supported by soft seals in the presence of internal and external pressure pulsations. International Journal of Heat and Mass Transfer 45, 5107–5115.

Langlois, W.E., 1962. Isothermal squeeze films. Quarterly of Applied Mathematics XX, 131–150.

Lavrik, N.V., Tipple, C.A., Sepaniak, M.J., Datskos, D., 20011,. Gold nano-structure for transduction of biomolecular interactions into micrometer scale movements. Biomedical Microdevices 3, 35–44.

Navier, C.L.M.H., 1823. Memoirs of the Academy of Science Institute, France 1, 414–416.

Pritchard, W.F., Davis, P.F., Derafshi, Z., Polacek, D.C., Tsoa, R., Dull R, .O., Jones, S.A., Giddens, D.P., 1995. Effects of wall shear stress and fluid recirculation on the localization of circulating monocytes in a three dimensional flow model. Journal of Biomechanics 28, 1459–1469.

Raiteri, R., Butt, H.-J., Grattarola, M., 2000. Changes in surface stress at the liquid/solid interface measured with a microcantilever. Electrochimica Acta 46, 157–163.

Shiping, Y., Ameel, T.A., 2001. Slip-flow heat transfer in rectangular microchannels. International Journal of Heat and Mass Transfer 44, 4225–4234.

Watanabe, K., Udagawa, H., 2001. Drag reduction of non-Newtonian fluid in a circular pipe with a highly water repellent wall. A.I.Ch.E. Journal 47, 256–262.

Wu, G., Datar, R.H., Hansen, K.M., Thundat, T., Cote, R.J., Majumdar, A., 2001. Bioassay of prostate-specific antigen (PSA) using microcantilever. Nature Biotechnology 19, 856–860.